

Next steps in aerostructural design of ultra-high aspect ratio wings

Yiyuan Ma*[†] and Ali Elham**

* *Bauhaus Luftfahrt e.V, Willy-Messerschmitt-Straße 1, 82024 Taufkirchen, Germany*

Yiyuan.Ma@bauhaus-luftfahrt.net

** *University of Southampton, Burgess Road, Southampton, Hampshire SO16 7QF, UK*

A.Elham@soton.ac.uk

[†] Corresponding Author

Abstract

This paper presents the authors' research work on the aerostructural design of Ultra-High Aspect-ratio Wings (UHARW). Firstly, aircraft configurations suitable for UHARW, especially unconventional configurations, are introduced and discussed. Then the aircraft conceptual design and analysis framework developed for the unconventional UHARW aircraft is described. The UHARW of the conceptually designed Strut-Braced Wing (SBW) and twin-fuselage aircraft are further investigated by employing a series of nonlinear aerostructural optimization methods, including the influences of aileron design and flutter constraint on the ultra-high aspect-ratio SBW design.

1. Introduction

Global air transportation is experiencing rapid growth and is expected to continue expanding in the coming decades. Boeing predicts a 4.0% annual growth in average traffic for the next 20 years, resulting in a need for more than 43,000 aircraft deliveries by 2040 [1]. Similarly, Airbus forecasts a 3.9% annual growth in revenue passenger kilometers, which will drive demand for over 39,000 new aircraft in the next 20 years [2]. Therefore, it is imperative to make substantial advancements in aircraft performance in order to mitigate the environmental impact of air transportation. Among the key strategies, the adoption of Ultra-High Aspect Ratio Wings (UHARW) configuration emerges as a promising option to achieve this goal.

The utilization of UHARW offers a viable solution for reducing induced drag, which can account for 40% of the total aircraft drag in an aircraft comparable to the A320 [3]. Thus, the development and progression of UHARW technology, along with associated airframe configurations, represent a pivotal strategy in enhancing fuel efficiency and mitigating emissions for the next-generation transport aircraft.

While the UHARW concept offers the advantage of lower induced drag, which reduces fuel consumption and increases range, it also poses challenges due to the significant aerodynamic load-induced wing bending moment and shear force. These factors result in increased structural weight, limiting the overall benefits of UHARW design. Recent research has explored alternative approaches to the UHARW concept, such as Strut-Braced Wings (SBW), Twin-Fuselage (TF) configurations, wingtip coupling, and folding wings [4–7]. However, the practical implementation of the UHARW design faces hurdles related to certification, technological constraints, and operational limitations. Complex aeroelastic behavior, manufacturing constraints, and dimensional restrictions imposed by airport infrastructure further complicate the viability of a fully deployable UHARW solution. Nevertheless, advancements in physics-based aircraft conceptual design tools and Multidisciplinary Design Optimization (MDO) methods, facilitated by increased computational power, offer the potential for developing unconventional solutions with novel and sustainable technologies.

The authors have conducted a series of systematic studies on UHARW in previous studies. Semi-empirical weight estimation method for TF aircraft with UHARW was developed in Ref. [8]. Conceptual design and analysis framework for SBW and TF configurations with UHARW was established based on semi-empirical and analytical methods, and several different SBW and TF aircraft were designed and analyzed to assess the potential of these configurations with UHARW design [4,9], as shown in Figure 1. Furthermore, an aerostructural optimization method was developed and

applied for the UHARW, as presented in Refs. [10–13]. This paper aims to provide an overview of the potential of UHARW through conceptual design and aerostructural optimization. It summarizes the authors' previous research on UHARW, consolidating the authors' findings into a comprehensive analysis. The remaining sections of this paper are organized as follows: Section 2 evaluates potential aircraft configurations for UHARW applications. In Section 3, the conceptual design and analysis framework and study results are presented. Section 4 introduces the aerostructural optimization method and optimization studies on high aspect-ratio SBW and TF wings. A summary of our key findings is provided in Section 5 of this paper.



Figure 1: SBW and TF aircraft with UHARW [4]

2. UHARW aircraft configurations

The aeronautical community is aware that current conventional tube-and-wing configurations might not be able to meet the needs of next-generation transport aircraft designs that are highly efficient, or might not be the best option. As found by Calderon et al. [14], the optimal aspect ratio for the studied conventional aircraft is about 18 to 19, when considering the optimum Breguet range. Karpuk and Elham also found that the optimal aspect ratio for cantilevered forward-swept and swept-back wings is about 16, when considering minimum direct operating cost.

Since unconventional aircraft configurations have the potential to yield significant gains in the medium term, justifying the risk and expense of their development, some efforts have therefore been made in recent years to investigate the potential of the UHARW concept with unconventional aircraft configurations. The authors have justified that the SBW and TF configurations are two promising concepts for implementing UHARW design while minimizing the structural weight penalty imposed by the ultra-high wing aspect ratio, and therefore a conceptual design and comparative study of SBW and TF aircraft with UHARW have been conducted by the authors [4]. As illustrated in Figure 1, the bending moment at the wing root is significantly reduced by utilizing an additional strut or the off-centreline located fuselages. The ideal configuration design is complicated by the coupling issue between the aerodynamics and structures of these two configurations. However, SBW and TF aircraft are less expensive and riskier than other disruptive aircraft configurations like blended-wing-body because they are based on the present conventional aircraft designs, including the fuselage, tailplanes, engines, etc.

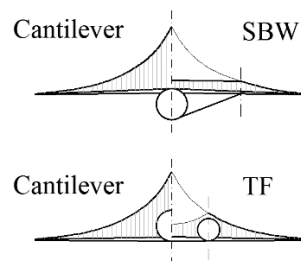


Figure 2: Wing bending moment comparison between cantilever wing and unconventional wings

3. Conceptual design of UHARW aircraft

This section describes the conceptual design environment developed by the authors in the previous work for the UHARW aircraft, followed by the conceptual design and comparative study results.

3.1 Conceptual design environment

The conceptual design and analysis environment developed by the authors for UHARW aircraft research is shown in Figure 3. The procedure starts with the initial sizing module employing PyInit [15], which is an in-house aircraft initial sizing tool developed for advanced transport aircraft initial sizing and performance evaluation. PyInit includes a wide variety of semi-empirical formulas and physics-based analytical techniques for constraint diagram sizing, component sizing, aerodynamic analysis, static stability, propulsion sizing, flight performance evaluation, etc., and PyInit has been modified for the SBW and TF aircraft initial sizing studies [4]. After the initial sizing by utilizing PyInit, the aircraft's thrust-to-weight ratio, wing loading, and component geometries are obtained. The initially sized aircraft is then entered into the mission analysis module for iterative calculations, where SUAVE, an open-source aircraft assessment tool created by Stanford University [16], is used to modify the aircraft geometry and weight to meet the mission segment requirements. It should be mentioned that the SUAVE has been modified by the authors to take into account the SBW and TF aircraft configurations. Specifically, a class-II wing weight estimation method for SBW aircraft developed by Chiozzotto [17] and a physics-based wing weight estimation method for TF aircraft developed by Udin and Anderson [9,18] have been integrated into the modified SUAVE for the unconventional UHARW aircraft performance analysis. In addition, OpenVSP [19] and CATIA were used for aircraft digital modeling and visualization.

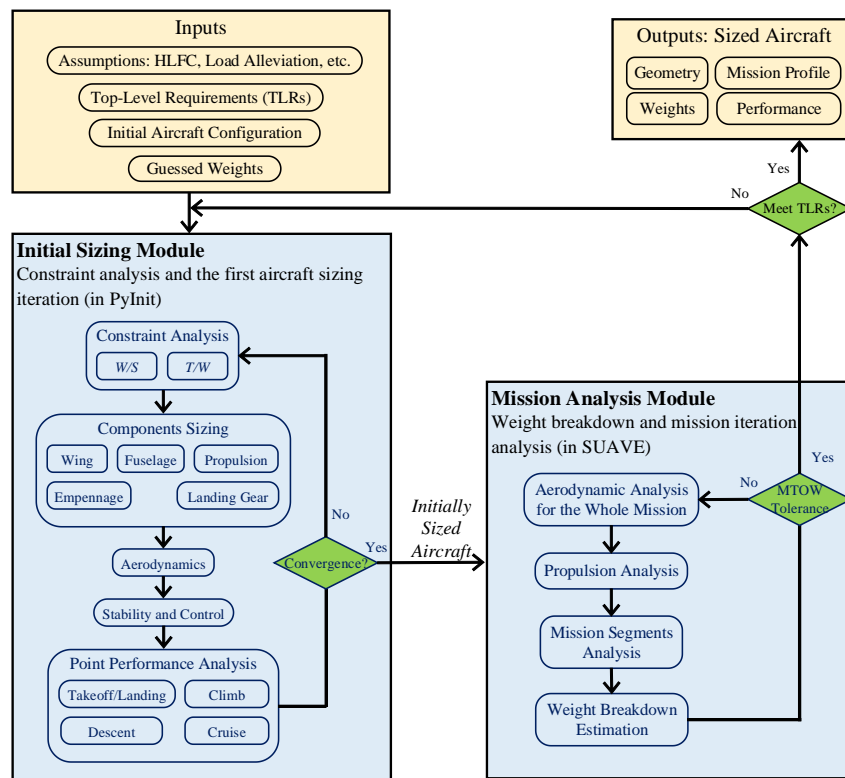


Figure 3: Conceptual design and analysis environment [4]

3.2 Conceptual design and comparative study

As given in Table 1, ATR-72-600, A320neo, and B777-300ER were selected as the reference aircraft for Short-Range (SR), Medium-Range (MR), and Long-Range (LR) missions, respectively. The entry-into-service was taken as the year 2040. The design mission profile of the aircraft is illustrated in Figure 4. The whole mission includes the main mission and a reserve segment. The current requirements for the reserve segment are 5% of trip fuel, a 200 nm diversion, and a 30 min hold. However, considering the designed UHARW aircraft will operate in the future scenario, these requirements are expected to be eased [20].

Table 1: Top-level aircraft requirements

| | Unit | SR | MR | LR |
|----------------------|------|--------|-------|-------|
| Reference Aircraft | -- | ATR-72 | A320 | B777 |
| Cruise Mach | -- | 0.42 | 0.78 | 0.84 |
| Max. Mach | -- | 0.457 | 0.82 | 0.89 |
| Passengers | -- | 72 | 150 | 350 |
| Range | nm | 825 | 3400 | 7500 |
| Cruise altitude | ft | 20000 | 33000 | 35000 |
| Service ceiling | ft | 25000 | 38500 | 40000 |
| Takeoff field length | ft | 4373 | 6400 | 9000 |
| Landing distance | ft | 3002 | 4500 | 9000 |
| Wingspan | m | 36 | 36 | 65 |

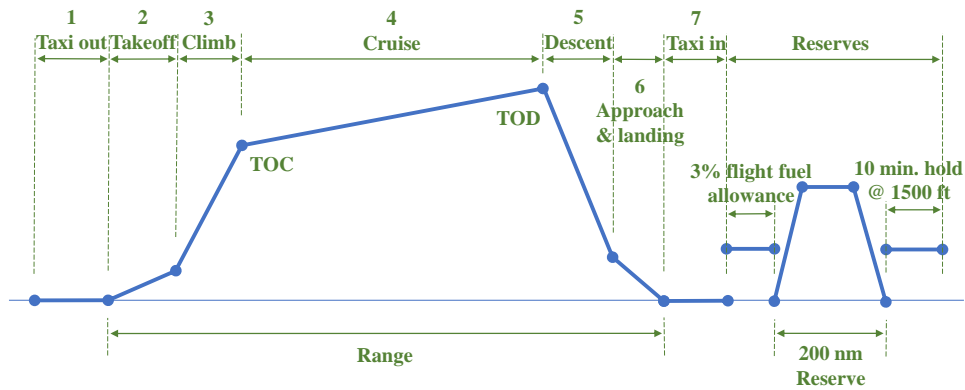


Figure 4: Design mission profile

The conceptual design and analysis environment shown in Figure 3 was utilized for the initial sizing and performance analysis of the SBW and TF aircraft for the SR, MR, and LR missions, respectively. The aircraft initial sizing tool PyInit was employed for the aircraft initial sizing. According to the top-level aircraft requirements and advanced technology assumptions (see Ref. [4]), the thrust-to-weight ratio and wing loading were determined based on the generated constraint diagram. Considering the UHARW design, both the SBW and TF configurations feature a high-wing configuration with two wing-mounted turbofan engines. The T-tail concept was chosen for the SBW and TF aircraft because of the high-wing configuration. The fuselage of the reference aircraft was utilized for the SBW aircraft and used as a guide for the TF aircraft's fuselage sizing. For example, the economy class on the MR A320neo has six-abreast seating. Due to the TF aircraft's smaller fuselage, the MR-TF aircraft's economy class seating is configured as four abreast to guarantee that the cabin size complies with the cabin design standards [21]. The sized cabin layout of the SR-TF and MR-TF aircraft are shown in Figure 5.

Next, the modified SUAVE was utilized to converge the aircraft weights while completing the defined flight missions. The flight conditions and aircraft configurations obtained from the initial sizing process were entered into SUAVE for iterative analysis. The Maximum Takeoff Weight (MTOW), fuel weight, and the empty weight of the converged SBW and TF aircraft for the SR, MR, and LR missions are given in Table 2. Both the SBW and TF aircraft with advanced airframe technologies show a significant advantage in fuel consumption and airframe weight over the reference aircraft for the three missions. For all the studied three missions, the TF configuration has a more significant weight reduction

effect on the wing structural weight than the SBW concept, making the MR-TF and LR-TF aircraft perform better than the SBW aircraft. However, due to the specific arrangement of the passenger cabin of the SR mission, the fuselage size had to be adjusted, resulting in heavier fuselages, and therefore the SR-SBW showed a better performance.

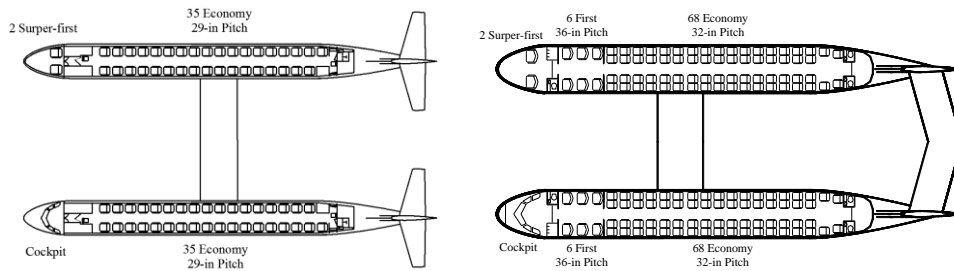


Figure 5: Fuselage interior arrangement of the SR- and MR-TF aircraft

Table 2: Weight data of the designed aircraft [4]

| | MTOW, kg | Fuel weight, kg | Empty weight, kg |
|------------|----------|-----------------|------------------|
| ATR 72-600 | 22800 | 2000 | 13500 |
| SR-SBW | 22229 | 1432 | 12821 |
| SR-TF | 22945 | 1523 | 13447 |
| A320neo | 79000 | 20980 | 44300 |
| MR-SBW | 67929 | 16127 | 37582 |
| MR-TF | 57777 | 13328 | 30229 |
| B777-300ER | 351535 | 145538 | 167829 |
| LR-SBW | 262962 | 89716 | 140066 |
| LR-TF | 210955 | 80037 | 97737 |

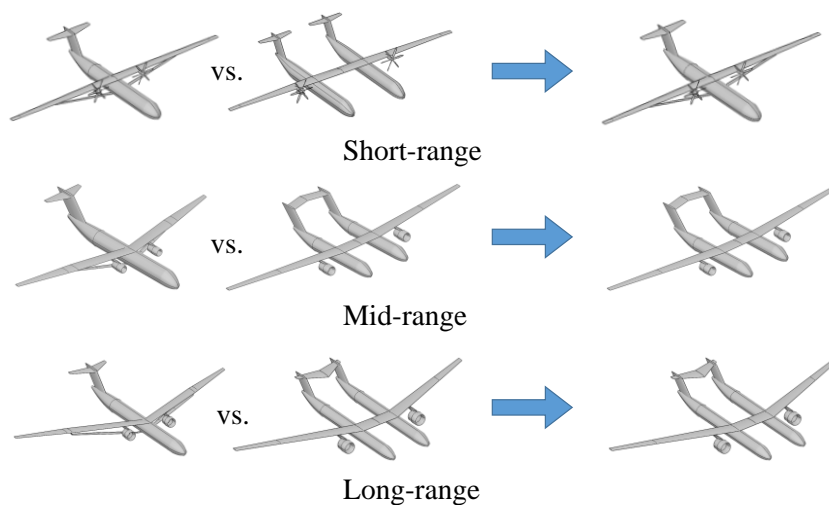


Figure 6: Conceptual design results

4. Aerostructural optimization of UHARW

This section presents the aerostructural optimization method developed by the authors and the optimization results for the high aspect-ratio SBW and TF wings.

4.1 Aerostructural optimization method

A coupled adjoint aerostructural wing optimization tool called FEMWET was created by Elham and van Tooren [22] and consists of a Quasi-Three-Dimensional (Q3D) aerodynamic solver and a finite beam element structural solver that is tightly coupled using the Newton method. In a recent study, Ma et al. [10] developed a geometrically nonlinear composite structural model and integrated it into FEMWET. In addition, the Q3D solver has also been adjusted to take the analysis and optimization of Natural Laminar Flow (NLF) into account.

The geometrically nonlinear structural method is based on composite thin-walled beams with assumptions specific to UHARW. The wing box is used to represent the wing cross-sections, and the large displacement analysis of composite thin-walled beams is taken into account when solving the finite element equations. A detailed description of the structural model can be found in Refs. [10,23].

The Q3D aerodynamic analysis method includes a Vortex Lattice Method (VLM) and the Two-Dimensional (2D) compressible airfoil analysis tool MSES [24]. The VLM code is used to calculate the wing lift coefficient, spanwise lift distribution, and induced drag. The Prandtl-Glauert compressibility adjustment is used to adjust the VLM calculation for the compressibility effect at a high Mach number. The wing is separated into various portions and subjected to 2D aerodynamic analysis with MSES to increase the accuracy of the analysis. By combining the results of the 2D aerodynamic study throughout the wingspan, the wing viscous, pressure, and wave drag are determined. The inviscid flow results are combined with compressible, integral boundary layer formulations that use the MSES edge velocity and envelop e^N boundary layer transition prediction criterion. Thus, MSES was used to project the laminar-to-turbulence transition point of the airfoil.

The given structural and aerodynamic solvers are combined to use the Newton method to resolve the coupled problem of flexible UHARW. Four governing equations were used to characterize the coupled aerostructural system, including the governing equations of the VLM and Finite Element Method (FEM), the governing equation for the level flight, and the equation for the Q3D method. For aerostructural optimization, a gradient-based optimization approach is employed. The coupled adjoint derivative calculation approach was employed for the sensitivity analysis to improve optimization efficiency.

The mission fuel weight was taken as the objective function in the optimization, which was estimated by utilizing the semi-empirical fuel weight estimation method presented by Roskam [25]. A more detailed description of the aerostructural optimization method and the validation can be referred to Ref. [10].

4.2 Wing aerostructural optimization study

The MR-SBW and MR-TF aircraft designed in the conceptual design phase (see Section 3) were employed for the mid-fidelity aerostructural optimization study. Both the SBW and TF aircraft were re-designed for the cruise Mach 0.735 as the reference configurations for the optimization according to the uncertainty analysis study conducted by the authors in Ref. [26].

In the aerostructural optimization, to ensure that the structure does not fail under tension, compression, and buckling loads of all the specified load conditions, restrictions were applied to the equivalent panels of the wing (and strut, for the SBW concept). The efficiency of the wing's aileron was also constrained to prevent aileron reversal. The weight of the primary and secondary wing components, as well as the weight of the wing box, was determined using the obtained equivalent panel thicknesses. The definition of the aerostructural optimization problem is:

$$\begin{aligned}
& \text{minimize} && W_F(X) \\
& \text{w.r.t.} && X = [t_{u_i}, t_l, t_{f_{s_i}}, t_{r_{s_i}}, G, P, W_{FS}, MTOW_S] \\
& \text{subject to} && \text{Failure}_k \leq 0 \\
& && 1 - L_{\delta} / L_{\delta, \min} \leq 0 \\
& && \frac{MTOW / S_w}{MTOW_0 / S_{w0}} - 1 \leq 0 \\
& && \frac{W_F}{W_{FA}} - 1 \leq 0 \\
& && \frac{W_F}{W_{FS}} - 1 = 0 \\
& && \frac{MTOW}{MOTW_S} - 1 = 0 \\
& && X_{lower} \leq X \leq X_{upper}
\end{aligned} \tag{1}$$

The design variables include the thickness of wing structural panels and spars, wing planform geometry, wing airfoil shapes, and two surrogate variables. The wing planform geometry includes wingspan, taper ratio, root chord, leading-edge sweep, and two twist angles at the kink and tip. To prevent further iterations between performance estimation and aerostructural analysis, two surrogate variables, i.e., fuel weight and MTOM, are defined.

The wing geometry and structure of the TF and SBW aircraft are illustrated in Figure 7 and Figure 8, respectively. The wing box is replaced by a beam placed at the elastic axis of the wing box. The equivalent beam is connected to the fuselage and the connection of the wing and the strut, and it has a fixed degree of freedom at the connection. The sequential quadratic optimization algorithm of the Matlab optimization toolbox was employed as the optimizer. For comparison purposes, the aerostructural optimization was performed in free transition mode, taking into account the flow transition of the wing starting with a transonic NLF airfoil, and in full turbulence mode (forced transition), for the wing starting with a supercritical airfoil. The optimization results of the TF wing and SBW are shown in Figure 9. The optimization of the TF wing in both free transition and full turbulence modes reduced the wing aspect ratio to decrease wing structural weight and the structural weight penalty due to the aileron effectiveness constraint. For both TF wing and SBW, the full turbulence aerostructural optimization reduced the wing aspect ratio and increased the wing sweep angle to decrease the wing structural weight and the total drag, especially the wave drag, thereby reducing the aircraft fuel weight. Whereas in the free transition mode, the optimizer decreased the wing sweep angle by reducing the wave drag by removing/weakening shock waves. In addition, the wing friction drag was reduced by more than 50% in the free transition mode optimization for both the TF wing and SBW because the wing airfoils were modified to widen the laminar flow boundary layer range on the wing [27]. In the optimization with boundary-layer free transition mode, the fuel weight of the TF aircraft was reduced by 13%, from 12638 kg to 10935 kg, and the MTOW was decreased from 56155 kg to 47758 kg [11]. In comparison, the optimizer reduced the fuel weight of the SBW aircraft from 16117 kg to 14406 kg, i.e., a 10% reduction; and the MTOW was reduced from 67262 kg to 61488 kg. The deflections of the optimized TF wing and SBW under a positive load condition are shown in Figure 10. The detailed optimization results and the comparison between these two configurations can be further referred to Ref. [11].

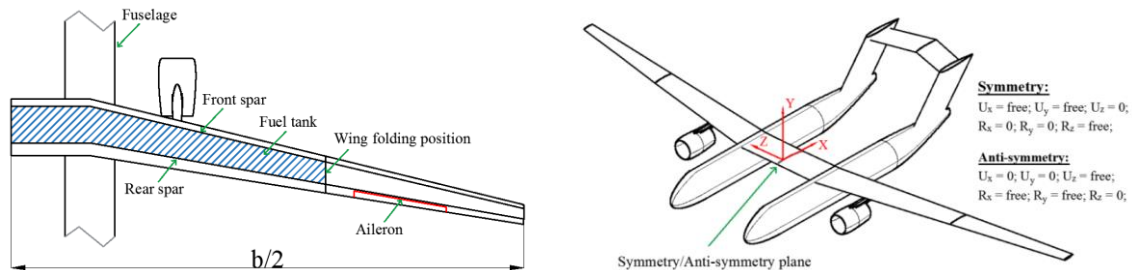


Figure 7: Schematic of TF wing (left) and example of wing beam model under positive load condition (right) [11]

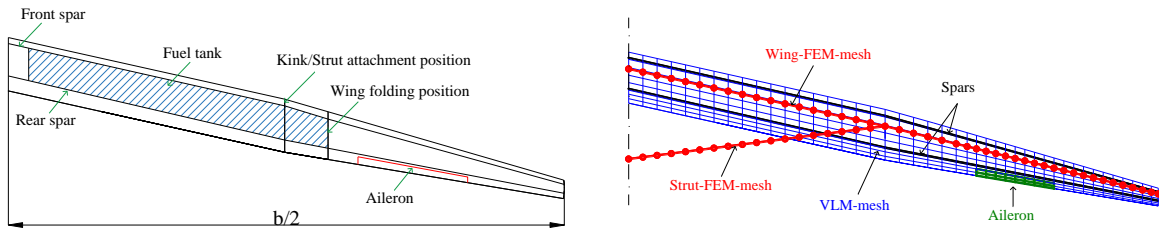
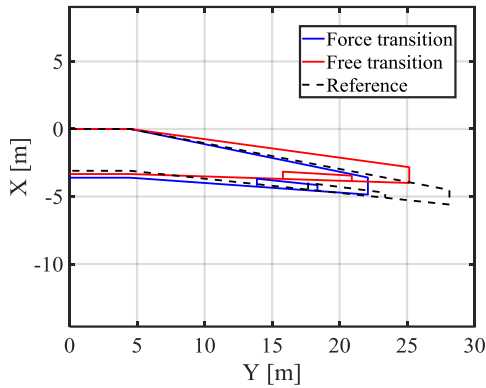
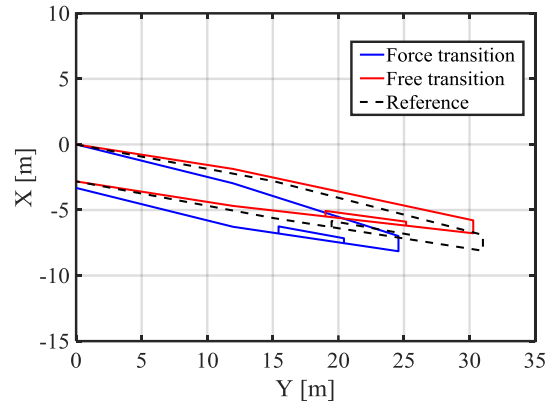


Figure 8: Schematic of SBW (left) and example of aerodynamic and structural mesh (right) [10]

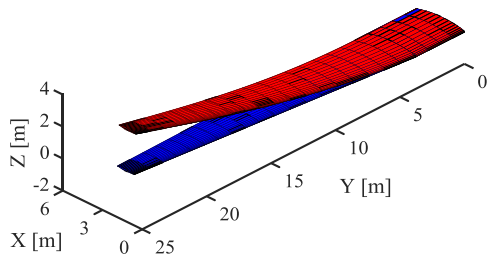


a) Optimized TF wing

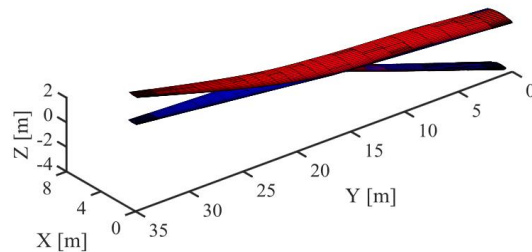


b) Optimized SBW

Figure 9: Wing planform comparison of the SBW and TF wing (force transition means the full turbulence boundary layer)



a) Optimized TF wing



b) Optimized SBW

Figure 10: Optimized wing's deflection under +1.5 g load condition [10,11]

Furthermore, the aileron design of the MR-SBW aircraft was also investigated. First, aeroelastic optimizations were performed for the SBW with and without the constraint of the aileron effectiveness. As shown in Figure 11, due to the combination of the not-high aspect ratio of the wing and the support of the strut, the influence of the aileron effectiveness constraint on the structural weight of the wings and struts is relatively negligible for the aspect ratio of 15 design. However, when the aspect ratio of wings grows, the aileron effectiveness constraint has a greater impact on the structural weight of the wings and struts. Additionally, as the wing aspect ratio rises, the structural weight of the wings increases more rapidly than the weight of the struts. Because the rolling moment caused by the aileron deflection is directly acting on the wing, it causes the wing structural weight increment to be more significant than that of the strut structural weight.

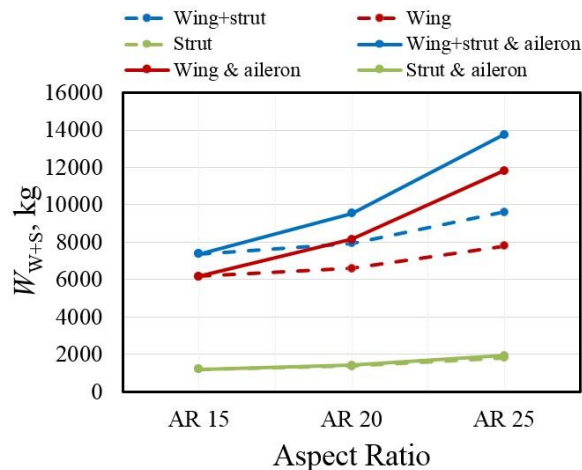


Figure 11: Structural weight of optimized SBW [27]

Aerostructural optimization of two different aileron configurations was conducted for the MR-SBW aircraft, including the single high-speed aileron concept and the low- and high-speed aileron concept, as shown in Figure 12. Ailerons are defined in FEMWET as devices that increase wing roll moment. The aileron placement and aileron geometry were added as design variables in the aerostructural optimization. As presented in Ref. [12], the optimized SBW with two ailerons had a 3% decrease in MTOW, a more than 8% decrease in fuel mass, and a more than 6% decrease in the mass of the wings and struts. While having a slightly stronger MTOW than the reference configuration, the optimized SBW with a single aileron shows a 5.5% fuel reduction.

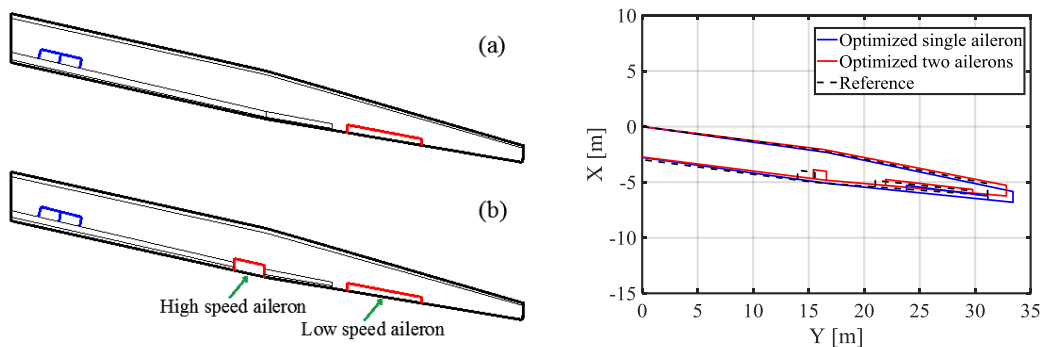


Figure 12: SBW aerostructural optimization results including aileron variables [12]

The wing structural weight data of SUGAR aircraft [6], which has a TBW configuration and a comparable wing aspect ratio, are utilized for comparison and reference purposes, as given in Table 3. It should be mentioned that the optimization results of the MR-SBW were obtained for the reduced load cases of $+1.5\text{ g}/-0.5\text{ g}$. As can be observed, the structural mass of the wing makes up roughly 80% of the entire structural mass (i.e., wing plus strut), while the structural mass of the strut makes up roughly 20% of the total structural mass.

For a more thorough comparison and reference, a series of aerostructural optimizations were carried out under conventional load conditions (i.e., $+2.5\text{ g}/-1.0\text{ g}$), and the SUGAR aircraft was employed as a comparison, as listed in Table 4. It is important to note that the fuel weight and MTOM of the aerostructurally optimized MR-SBW aircraft in free transition mode are comparable to those of the SUGAR aircraft, whereas those of the optimized MR-SBW aircraft in full turbulence mode are noticeably worse than the free transition mode case and the SUGAR aircraft due to its worse starting point and higher drag. The SUGAR aircraft applies the NLF wing design so it shows a better performance than the optimized MR-SBW in the full turbulence mode. In addition, the SUGAR aircraft utilizes fuselage riblets and airframe structural weight reduction assumptions that were not considered in the MR-SBW optimization, which allows the SUGAR aircraft to have fuel weight and MTOW comparable to the free-transition optimized MR-SBW, even with a relatively small wing aspect ratio.

Table 3: Wing mass breakdown and aileron effectiveness [10]

| Configuration | m_{w+s} , kg | m_w , kg | m_s , kg | m_w/m_{w+s} | m_s/m_{w+s} | η_a |
|----------------------|----------------|------------|------------|---------------|---------------|----------|
| Reference | 11418 | 8824.8 | 2593.2 | 0.77 | 0.23 | 0.381 |
| Full turbulence opt. | 7734.5 | 6072.6 | 1661.9 | 0.79 | 0.21 | 0.455 |
| Free transition opt. | 7823.8 | 6301.1 | 1522.7 | 0.81 | 0.19 | 0.502 |
| SUGAR [6] | 9230.6 | 7561.4 | 1669.2 | 0.82 | 0.18 | -- |

Table 4: Comparison of the MR-SBW and SUGAR aircraft (both under +2.5 g/-1.0 g load cases) [10]

| Configuration | Fuel, kg | MTOW, kg | m_{w+s} , kg | AR |
|---------------------------|----------|----------|----------------|-------|
| Reference turbulence | 22205 | 79944 | 14418 | 25.81 |
| Full turbulence opt. | 20128 | 76977 | 12526 | 17.70 |
| Reference free transition | 16523 | 72334 | 12422 | 25.81 |
| Free transition opt. | 14540 | 67340 | 10510 | 23.33 |
| SUGAR [6] | 14470 | 68039 | 9231 | 19.55 |

Since UHARW are more flexible and prone to flutter compared to conventional wings, the flutter analysis module needs to be integrated into the aerostructural optimization framework. The method developed by Mallik et al. [28] for rapid transonic flutter analysis with validation results for SBW was utilized. The transonic indicial functions in Mallik's method were combined with the geometrically nonlinear structural model of FEWMET, and the transonic corrections were directly applied to employ MSES results in the Q3D method of FEMWET. The code was fully differentiated to be integrated with coupled adjoint aerostructural optimization [13]. A constraint on flutter, i.e., the aggregated function of the damping ratios, was also specified to ensure that the optimized wing is flutter-free. The optimization was set to decrease the fuel mass while meeting the constraints on the wing structural failure, aileron effectiveness, wing loading, and flutter. The aerostructural optimization reduced the structural mass of the wing and strut by 7.4% and the aircraft fuel mass by more than 6%. In order to produce an optimal wing free of flutter inside the flight envelope, the optimizer improved the wing's stiffness and decreased the distance between the wing's sectional center of gravity and the elastic axis (see Figure 13).

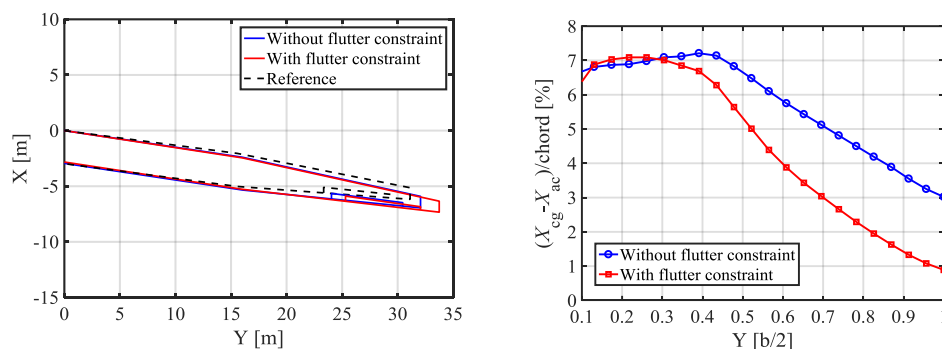


Figure 13: SBW aerostructural optimization with flutter constraint [13]

The results of the above mentioned a series of aerostructural optimizations conducted by the authors for the MR-SBW aircraft are compared in Table 5. The conceptual design outcomes were utilized as the starting point of aerostructural optimizations. The percentage changes given in the table clearly show the effect of the maximum load factors, aileron design parameters, and flutter constraints on the fuel mass, MTOW, and wing AR of the aircraft.

Table 5: Comparing the results of a series of aerostructural optimizations

| SBW configuration | Fuel mass, kg | MTOW, kg | AR |
|------------------------------|-----------------|----------------|-----------------|
| Conceptual design | 16117 | 67262 | 25.81 |
| Opt. with +2.5 g/-1.0 g | 14540 (-9.78%) | 67340 (+0.12%) | 23.33 (-9.61%) |
| Opt. with +1.5 g/-0.5 g | 14406 (-10.62%) | 61488 (-8.58%) | 26.01 (+0.77%) |
| Conceptual design | 16644 | 67623 | 25.00 |
| Opt. with aileron variables | 15202 (-8.66%) | 65639 (-2.93%) | 28.65 (+14.60%) |
| Opt. with flutter constraint | 15587 (-6.35%) | 69512 (+2.79%) | 28.52 (+14.08%) |

5. Conclusion

This paper summarized the authors' research on the aerostructural design of UHARW. It began by introducing and analyzing suitable aircraft configurations for UHARW, including unconventional concepts. A dedicated aircraft conceptual design and analysis framework was described, specifically tailored for unconventional UHARW aircraft.

Further investigations conducted on the wings of conceptually designed SBW and TF aircraft using a mid-fidelity aerostructural optimization method were described. This approach allowed for the exploration of various design parameters and constraints to enhance the performance and efficiency of UHARW wings. The influence of aileron design and flutter constraints on the ultra-high aspect-ratio SBW was studied.

This paper presented a systematic study describing approaches to address the challenges of aerostructural design in UHARW configurations. Avenues for future research include the integration of high-fidelity aerodynamic methods to take into account the effects of wing-strut interaction.

6. Acknowledgements

Some parts of the research presented in this publication were performed under the RHEA project. This project has received funding from the Clean Sky 2 Joint Undertaking (JU) under grant agreement no 883670. The JU receives support from the European Union's Horizon 2020 Research and Innovation Programme and the Clean Sky 2 JU members other than the Union.

References

- [1] *Commercial Market Outlook 2021-2040*. 2021. Boeing.
- [2] *Airbus Global Market Forecast 2021 - 2040*. 2021. Airbus.
- [3] Beck, N., Landa, T., Seitz, A., Boermans, L., Liu, Y., and Radespiel, R. 2018. Drag Reduction by Laminar Flow Control. *Energies*, Vol. 11, No. 1, p. 252.
- [4] Ma, Y., Karpuk, S., and Elham, A. 2022. Conceptual Design and Comparative Study of Strut-Braced Wing and Twin-Fuselage Aircraft Configurations with Ultra-High Aspect Ratio Wings. *Aerospace Science and Technology*, Vol. 121, p. 107395.
- [5] Gu, H., Healy, F., Rezgui, D., and Cooper, J. 2023. Sizing of High-Aspect-Ratio Wings with Folding Wingtips. *Journal of Aircraft*, Vol. 60, No. 2, pp. 461–475.
- [6] Bradley, M. K., K. Dorney, C., and Allen, T. 2015. *Subsonic Ultra Green Aircraft Research: Phase II – Volume I – Truss Braced Wing Design Exploration*. Publication NASA/CR–2015-218704/Volume I.
- [7] Ma, Y., Zhang, W., and Elham, A. 2022. Multidisciplinary Design Optimization of Twin-Fuselage Aircraft with Boundary-Layer-Ingesting Distributed Propulsion. *Journal of Aircraft*, Vol. 59, No. 6, pp. 1588–1602.
- [8] Ma, Y., Yan, J., and Elham, A. 2023. Initial Weight Estimation of Twin-Fuselage Configuration in Aircraft Conceptual Design. *Proceedings of the Institution of Mechanical Engineers, Part G: Journal of Aerospace Engineering*, Vol. 237, No. 1, pp. 130–140.

- [9] Ma, Y., and Elham, A. 2021. Twin-Fuselage Configuration for Improving Fuel Efficiency of Passenger Aircraft. *Aerospace Science and Technology*, Vol. 118, p. 107000.
- [10] Ma, Y., Abouhamzeh, M., and Elham, A. 2022. Geometrically Nonlinear Coupled Adjoint Aerostructural Optimization of Natural-Laminar-Flow Strut-Braced Wing. *Journal of Aircraft*, pp. 1–20.
- [11] Ma, Y., Abouhamzeh, M., and Elham, A. 2023. Aerostructural Optimization and Comparative Study of Strut-Braced-Wing and Twin-Fuselage Aircraft Configurations with Ultra-High Aspect Ratio Wings. Presented at the *AIAA SCITECH 2023 Forum*, National Harbor, MD & Online.
- [12] Ma, Y., Abouhamzeh, M., and Elham, A. 2023. Investigating Aileron Design for Ultra-High Aspect Ratio Wings. Presented at the *AIAA SCITECH 2023 Forum*, National Harbor, MD & Online.
- [13] Ma, Y., Abouhamzeh, M., Da Ronch, A., and Elham, A. 2023. Geometrically Nonlinear Coupled-Adjoint Aerostructural Optimization of Ultra-High Aspect Ratio Wings with Flutter Constraints. Presented at the *AIAA SCITECH 2023 Forum*, National Harbor, MD & Online.
- [14] Calderon, D. E., Cooper, J. E., Lowenberg, M., Neild, S. A., and Coetzee, E. B. 2019. Sizing High-Aspect-Ratio Wings with a Geometrically Nonlinear Beam Model. *Journal of Aircraft*, Vol. 56, No. 4, pp. 1455–1470.
- [15] Karpuk, S., and Elham, A. 2021. Conceptual Design Trade Study for an Energy-Efficient Mid-Range Aircraft with Novel Technologies. Presented at the *AIAA Scitech 2021 Forum*, VIRTUAL EVENT.
- [16] Lukaczyk, T. W., Wendorff, A. D., Colonno, M., Economon, T. D., Alonso, J. J., Orra, T. H., and Ilario, C. 2015. SUAVE: An Open-Source Environment for Multi-Fidelity Conceptual Vehicle Design. Presented at the *16th AIAA/ISSMO Multidisciplinary Analysis and Optimization Conference*, Dallas, TX.
- [17] P. Chiozzotto, G. 2017. Initial Weight Estimate of Advanced Transport Aircraft Concepts Considering Aeroelastic Effects. Presented at the *55th AIAA Aerospace Sciences Meeting*, Grapevine, Texas.
- [18] Udin, S. V., and Anderson, W. J. 1992. Wing Mass Formula for Twin Fuselage Aircraft. *Journal of Aircraft*, Vol. 29, No. 5, pp. 907–914.
- [19] McDonald, R. A. 2016. Advanced Modeling in OpenVSP. Presented at the *16th AIAA Aviation Technology, Integration, and Operations Conference*, Washington, D.C.
- [20] Greitzer, E. M., Bonnefoy, P. A., Hall, D. K., Hansman, R. J., Hileman, J. I., Liebeck, R. H., Lovegren, J., Mody, P., Pertuze, J. A., Sato, S., Spakovszky, Z. S., Tan, C. S., Hollman, J. S., Duda, J. E., Fitzgerald, N., Houghton, J., Kerrebrock, J. L., Kiwada, G. F., Kordonowy, D., Parrish, J. C., Tylko, J., and Wen, E. A. 2010. N+3 Aircraft Concept Designs and Trade Studies, Final Report. *Final Report*, Vol. 1.
- [21] Torenbeek, E. 2013. *Advanced Aircraft Design: Conceptual Design, Analysis, and Optimization of Subsonic Civil Airplanes*. Wiley, Chichester.
- [22] Elham, A., and van Tooren, M. J. L. 2016. Coupled Adjoint Aerostructural Wing Optimization Using Quasi-Three-Dimensional Aerodynamic Analysis. *Structural and Multidisciplinary Optimization*, Vol. 54, No. 4, pp. 889–906.
- [23] Abouhamzeh, M., Ma, Y., and Elham, A. 2022. A Geometrically Nonlinear Structural Model For Aerostructural Optimization of Ultra-High Aspect Ratio Composite Wings. Presented at the *AIAA SCITECH 2022 Forum*, San Diego, CA & Virtual.
- [24] Drela, M. 2007. *MSES: Multi-Element Airfoil Design/Analysis Software*. Publication Ver. 3.07. Massachusetts Institute of Technology.
- [25] Roskam, J. 1997. *Airplane Design, Part I: Preliminary Sizing of Airplanes*. Design, Analysis and Research Corporation, Lawrence, Kansas.
- [26] Ma, Y., Minisci, E., and Elham, A. 2021. INVESTIGATING THE INFLUENCE OF UNCERTAINTY IN NOVEL AIRFRAME TECHNOLOGIES ON REALIZING ULTRA-HIGH ASPECT RATIO WINGS. Presented at the *AeroBest 2021*.
- [27] Ma, Y. 2022. *Design and Optimization for Unconventional Aircraft Configurations with Ultra-High Aspect Ratio Wings*. Technischen Universität Braunschweig, Braunschweig, Germany.
- [28] Mallik, W., Schetz, J. A., and Kapania, R. K. 2018. Rapid Transonic Flutter Analysis for Aircraft Conceptual Design Applications.” *AIAA Journal*, Vol. 56, No. 6, pp. 2389–2402.